

Biophotonic techniques for the study of malaria-infected red blood cells

Jakob M. A. Mauritz · Alessandro Esposito · Teresa Tiffert ·
Jeremy N. Skepper · Alice Warley · Young-Zoon Yoon ·
Pietro Cicuta · Virgilio L. Lew · Jochen R. Guck · Clemens F. Kaminski

Received: 17 May 2010/Accepted: 11 July 2010/Published online: 27 July 2010
© International Federation for Medical and Biological Engineering 2010

Abstract Investigation of the homeostasis of red blood cells upon infection by *Plasmodium falciparum* poses complex experimental challenges. Changes in red cell shape, volume, protein, and ion balance are difficult to quantify. In this article, we review a wide range of optical techniques for quantitative measurements of critical homeostatic parameters in malaria-infected red blood cells. Fluorescence lifetime imaging and tomographic phase microscopy, quantitative deconvolution microscopy, and X-ray microanalysis, are used to measure haemoglobin concentration, cell volume, and ion contents. Atomic force microscopy is briefly reviewed in the context of these optical methodologies. We also describe how optical tweezers and optical stretchers can be usefully applied to empower basic malaria research to yield diagnostic information on cell compliance changes upon malaria infection. The combined application of these techniques sheds new light on the detailed mechanisms of malaria infection

providing potential for new diagnostic or therapeutic approaches.

Keywords Malaria · *Plasmodium falciparum* · FLIM · FRET · Optical tweezers · Optical stretcher · Haemoglobin concentration · X-ray microanalysis · Micropositioning · EDS · EPXMA · Red cell model · AFM

1 Introduction

Malaria is a mosquito-borne disease that affects more than 350 million people per year. The most severe form of human malaria is caused by the protozoan parasite *Plasmodium falciparum*. After an initial incubation period in liver cells, the parasites invade red blood cells (RBCs), using them as hosts for their 48-h asexual reproductive

J. M. A. Mauritz · A. Esposito · C. F. Kaminski (✉)
Department of Chemical Engineering and Biotechnology,
University of Cambridge, Pembroke Street,
Cambridge CB2 3RA, UK
e-mail: cfk23@cam.ac.uk

J. M. A. Mauritz · A. Esposito · T. Tiffert ·
J. N. Skepper · V. L. Lew
Department of Physiology, Development and Neuroscience,
University of Cambridge, Cambridge, UK

A. Warley
Centre For Ultrastructural Imaging, King's College London,
London, UK

Y.-Z. Yoon · P. Cicuta · J. R. Guck
Sector of Biological and Soft Systems, Cavendish Laboratory,
Department of Physics, University of Cambridge,
Cambridge, UK

Y.-Z. Yoon
Department of Physics, Sungkyunkwan University,
Suwon 440-746, Korea

P. Cicuta
Nanoscience Center, University of Cambridge, Cambridge, UK

C. F. Kaminski
School for Advanced Optical Technologies, Friedrich-Alexander-Universität Erlangen-Nürnberg, Erlangen, Germany

Present Address:
A. Esposito
MRC Cancer Cell Unit, Hutchison/MRC Research Centre, Hills Road, Cambridge CB20XZ, UK

cycle. This cycle progresses through several stages; at first, merozoites released from liver cells into the blood stream invade red blood cells. This is followed by a relatively quiescent ring-stage (named after the characteristic parasite shape) for up to 16–20 h post-invasion. During the following trophozoite stage, the glycolytic metabolism of the infected red blood cell (IRBC) increases a hundred-fold; the permeability of the host cell membrane is also increased by several orders of magnitude by the activation of new permeability pathways (NPPs) [29]. The non-selective NPPs allow for an increased diffusive flux of nutrients, metabolic waste products, and ions. Haemoglobin (Hb) ingestion and digestion begin shortly after the onset of NPPs [15, 31]. Ultimately, up to 80% of the host cell haemoglobin is degraded. More than 80% of the aminoacids produced in the process are released as waste through the NPPs, thus only a minimal fraction of amino-acids are used for de novo protein synthesis. In the final schizont stage, at about 40–48 h post-invasion, the parasite segments and finally ruptures the host cell, releasing 20–30 new merozoites for infection of other, uninfected RBCs. These developments cause dramatic changes in the homeostasis of IRBCs, affecting key homeostatic parameters, such as membrane permeability and transmembrane transport, ion and protein content, rheological properties, cell shape and volume [29]. The large number of parameters, their complex interconnections and their relation to the overall homeostatic behavior of red blood cells upon infection present a formidable challenge both to cell modelers, who aim to develop predictive capabilities for blood cell homeostasis, and to experimentalists, in their effort to provide quantitative data for use as model input and validation. There has been much recent interest in this area of malaria research in which the application of state-of-the-art optical, imaging and X-ray microanalytical methods has made it possible to solve long-standing open questions on the homeostatic behavior of RBCs upon infection [4, 21, 36, 41, 53], and have also made accessible further areas of enquiry in this disease. In what follows we present different methods used for non-invasive and functional imaging of IRBCs and present examples of how these methods help our theoretical understanding from modeling. The emphasis is on novel experimental techniques, and their promise for applications in basic malaria research.

2 Non-invasive imaging of RBCs

2.1 Wide-field and confocal laser scanning microscopy

Wide-field differential interference contrast (DIC) and fluorescence microscopy are the classical “workhorses”

used for studying live IRBCs. Optical microscopy permits the non invasive imaging of IRBC, the study of parasite development [22], mapping the localization of proteins [57], or characterizing alterations of host cell morphology [16]. Chemical and laser-light toxicity is known to occur, but protocols for minimizing these problems have been characterized [21, 56]. Wide-field imaging of IRBC has been extraordinarily successful in investigating RBC invasion and merozoite release processes. Glushakova et al. used time-lapsed imaging for recording RBC membrane transformations during merozoite egress [21, 22]. Their results showed that immediately prior to rupture IRBC morphology changes into a near-spherical configuration and helped distinguish between different hypothetical models of merozoite egress.

More precise imaging can be achieved by employing a confocal laser scanning microscope (CLSM) combined with fluorescence techniques and fluorophore-loaded cells. This allows non invasive volumetric imaging of biological samples. A confocal microscope produces sharp optical sections by removing out-of-focus image blur through the use of a pinhole positioned in front of the detector. The resolution of a typical CLSM equipped with a high numerical aperture objective is about 200–250 nm laterally and 500–700 nm along the optical axis for a green fluorophore. Each optical section is acquired by scanning the laser in the sample plane with galvanometric mirrors; a number of optical sections are then acquired by sweeping the focal plane of the microscope through the sample. The image stacks are subsequently deconvolved to further improve resolution [6] and this can be applied to measure cell volumes and surface areas.

A variation to this setup is the use of an array of pinholes rapidly scanned in front of a wide field detector such as in Nipkov-disk based confocal microscopes. Tokumasu and Dvorak combined the high 3D resolution of a Nipkov-disk confocal with labeling fixed IRBCs with quantum dots, fluorophores that circumvent the common problem of rapid photobleaching observed with classical fluorophores [56, 57]. In their study, the quantum dots were used to immuno-label the membrane protein band 3 and image the host cell membrane deformations during merozoite invasion. They were also able to map the distribution of Band 3 which surprisingly occurred inhomogeneously clustered on the erythrocyte membrane [57].

Examples of three-dimensional images obtained with CLSM are shown in Fig. 1. Here, live IRBC were labeled with the organic fluorophore calcein [16] and embedded in agarose gel. These images are examples of 3D volume reconstructions of uninfected (Fig. 1a) and infected (Fig. 1b) RBCs. Quantitative volume estimates depend

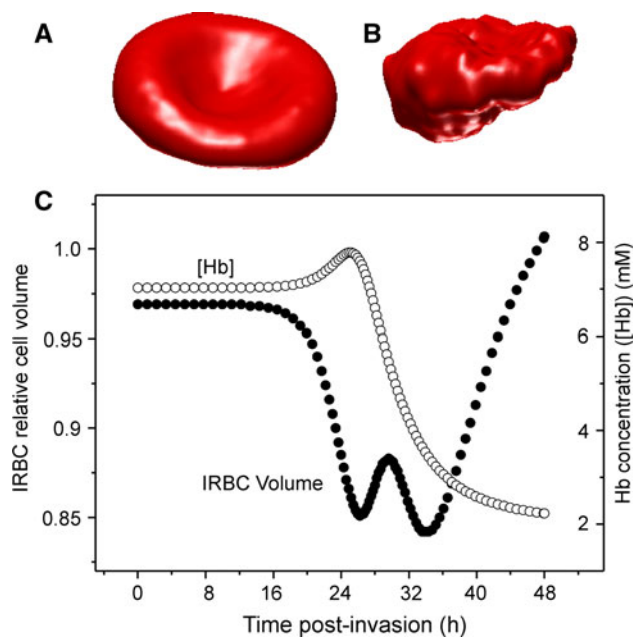


Fig. 1 (a, b) Example of 3D volume reconstructions of an uninfected RBC (a) and trophozoite IRBC (b). (c) Simulated Hb concentration and IRBC volume, assuming that the parasite grows by about 30% for any volume unit of ingested cytosol [41]

critically on the segmentation algorithm applied on the image objects, calcein-loaded RBCs in this example. In order to minimize bias present in traditional methods, special algorithms can fit the object-to-background intensity transition along the normal of an initial iso-surface. The method works by connecting all pixels of the 3D image stack that exhibit an arbitrary intensity value (guessing an intensity at the boundary) and fitting an error function locally to the intensity profile perpendicular to this surface. The initial surface is then elastically deformed towards the inflection points of the fit. Simulations show that this algorithm can achieve a volume accuracy of less than 5 fl [16]. With this method it was shown that IRBCs have a slightly increased mean volume at the trophozoite stage (25–40 h post invasion), and a slightly smaller mean volume than uninfected RBCs at the schizont stage (40–48 h post-invasion) [16].

The various studies described above provide the latest insight into all stages of infection, from the invasion process, through parasite maturation, and merozoite release. From these data it becomes clear that a pre-terminal near spherical host morphology with IRBC volumes similar to uninfected RBCs can only be reconciled if the membrane area of IRBCs is significantly reduced during the infection. The homeostatic IRBC model is compatible with this terminal condition if it is assumed that the parasite grows only by about 30% for any volume unit of ingested cytoplasm (Fig. 1c) [4, 14, 15, 51, 61].

2.2 Tomographic phase microscopy

Volumetric information of IRBCs can be obtained non-invasively also by tomographic phase microscopy (TPM) [8, 46]. This interferometric technique sweeps the illumination angle of the sample in a microscope, similar to computer assisted X-ray tomography, and collects images of the optical phase information. Multiple acquisitions from different angles can then be used to reconstruct a volumetric image with the filtered back-projection method (inverse Radon transform). The transversal/longitudinal spatial resolution of the technique is limited to 0.3 and 0.6 μm , respectively [8]. Furthermore, the optical phase information can be used to calculate refractive index maps of the sample. TPM is an elegant non-invasive technique that does not rely on cytosol staining, but makes use of refractive index differences in the cell.

Park et al. have used this technique to gather 3D tomographic maps of IRBCs. They have then calculated host cytosol volumes by subtracting the parasite from the total IRBC volume. In the different developmental stages of the IRBC they report host cell volumes of 93.1 ± 7.9 fl, 88.5 ± 11.8 fl, 57.5 ± 13.8 fl, and 34.2 ± 15.1 fl for uninfected, ring stage, trophozoite and schizont stage IRBCs, respectively.

Tomographic phase microscopy was also used to estimate the prevailing Hb concentration from the refractive index, on the assumption that Hb is the main contributor to the refractive index change. The accuracy of the refractive index estimates from the optical phase information is reported as 0.001 [8]. Hb concentrations in the various developmental stages have been measured as 7.0 ± 0.5 mM, 6.5 ± 0.4 mM, 4.9 ± 0.4 mM, and 3.8 ± 0.5 mM for uninfected, ring stage, trophozoite stage and schizont stage IRBCs, respectively. However, the relatively large voxel volume (roughly $0.3 \times 0.3 \times 0.6 \mu\text{m}^3$) may cause the measurements to be affected by the presence of Hb-free domains within the host cytosol, such as vesicles surrounded by parasitophorous vacuolar membrane, which could generate bias towards lower concentrations of Hb in the host cytosol.

2.3 Atomic force microscopy

Although this review is focused on optical techniques, atomic force microscopy (AFM) is another widely used method for the imaging of morphological changes in IRBCs worth mentioning. AFM measures the deflection of a cantilever equipped with a sharp tip (the probe). While scanning the probe in close proximity to the sample, AFM maps the topology of surfaces by sensing (depending on the mode of operation and on the probe) a variety of forces, e.g., van der Waals, electrostatic, magnetic forces, etc.

[19, 28]. AFM can provide atomic resolution, but the spatial resolution for biological samples is usually limited to 50 nm [19, 44]. In malaria research AFM was used to observe a positive surface charge on IRBC specific membrane knobs—causative for the strong cytoadherence of IRBCs [1, 2, 43]. The number of IRBC membrane knobs was found to be directly proportional to the number of parasites in the host cell, and the knob volume was found to be constant throughout parasite maturation [43]. Similarly, the apical end of merozoites was found to be positively charged, which is believed to play a key role in the merozoite alignment and RBC invasion process [3]. Finally AFM was used to image the changes in RBC cytoskeleton morphology during parasite maturation [20].

3 Functional imaging in infected-RBCs

3.1 Ratiometric imaging

Organic fluorophores that are sensitive to their chemical environment are now widely available. Typically, the presence of the molecule to be quantified induces conformational changes in the dye. This can in turn change the emission spectrum of the fluorophore. A change in the concentration of the molecule of interest can thus be quantified by comparing the area of different emission peaks in the fluorophore spectrum (ratiometric imaging). This technique has been used in malaria research to quantify differences in acidity in chloroquine resistant and non-resistant parasite strains with pH sensitive dyes (e.g., pHluorin in [32]) or to assess Ca^{2+} accumulation in the parasite food vacuole with a Ca-sensitive dye (e.g., Fura Red in [49]). The selection of the dye requires careful attention and planning, as some “standard” ratiometric dyes for RBCs can be phototoxic for the parasite [49].

3.2 Fluorescence lifetime imaging

Förster Resonance Energy Transfer (FRET) [12] occurs when an optically excited donor molecule is close (typically less than 10 nm) to an acceptor molecule with an efficiency that decays with the inverse of the 6th power of the distance between donor and acceptor [27]. The non-radiative energy transfer quenches the fluorescence intensity and lifetime of the donor and can be used to quantitatively image the presence or interactions between donor and acceptor molecule. This technique is particularly well suited for quantifying intracellular concentrations, observing molecular interaction or post-translational modifications. In malaria research, FRET has been used for genotyping resistance related mutations [42], observing the targeting of ligands or inhibitors to the parasite [9, 10] or

for rapid differentiation between different Plasmodium species [50].

FRET shortens the lifetime of the optically excited state. Fluorescence lifetime imaging (FLIM) quantifies the fluorophore lifetimes for each microscope image pixel by counting photon arrival times (time domain FLIM [47]) or detecting phase delays with respect to the modulation of the excitation light (frequency domain FLIM [13]). Esposito et al. used time domain FLIM to measure Hb concentrations in IRBCs, after loading them non-disruptively with the dye calcein-AM [17]. The physiological Hb molecular crowding is so high that any fluorophore in the cytosol is only a few nanometers away from multiple heme moieties. This causes FRET from calcein to the neighboring Hb molecules, as the absorption spectrum of Hb shows significant overlap with the calcein emission spectrum. Figure 2a shows confocal sections of two uninfected cells and Fig. 2c of one infected cell with a trophozoite-stage parasite. Figure 2b, d show the corresponding FLIM images. The healthy cells shown in Fig. 2b display a lifetime of 280 ± 30 ps (top cell) and 260 ± 30 ps (bottom cell) which increases to 950 ± 200 ps in the IRBC host cytoplasm and 2.6 ± 0.2 ns in the parasite compartment, indicative of dequenching as the Hb concentration is decreased. Calibrated against RBC haemolysates, these values correspond to Hb concentrations of 7.0 ± 0.4 mM

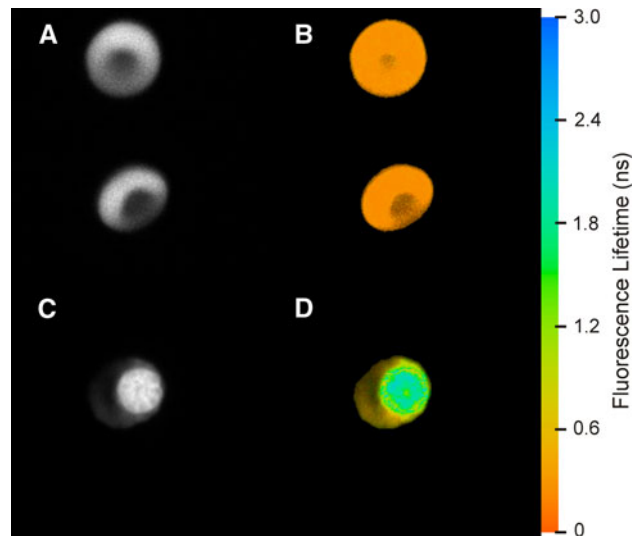


Fig. 2 Intensity (**a**, **c**) and Fluorescence lifetime (**b**, **d**) images of RBCs during *P. falciparum* infection, recorded by confocal microscopy. The colourmap represents lifetimes from 0 to 3 ns. The averaged lifetime of an uninfected cell (**b**) is 280 ± 30 ps (*top*) and 260 ± 30 ps (*bottom*). The IRBC trophozoite (**d**) has an increased average lifetime of 950 ± 200 ps in the host cytoplasm and 2.6 ± 0.2 ns in the parasite compartment. The short fluorescence lifetime observed in uninfected cells is due to the high degree of energy transfer occurring between hemoglobin and the fluorescent dye, which upon calibration provides a measure of intracellular Hb concentration [17]

and 7.3 ± 0.4 mM for uninfected cells, of 2.95 ± 0.45 mM for the host cell cytoplasm and of 0.75 ± 0.16 mM for the parasite cytoplasm [17]. These values are in good agreement with the results obtained by the TPM method confirming the predictions of the homeostatic IRBC model shown in Fig. 1c [17].

3.3 Electron probe X-ray microanalysis

Electron probe X-ray microanalysis (EPXMA) is a well-established technique for the quantification of intracellular elements such as Na, K, Cl, Ca, S, P, and Fe [18]. In an electron microscope, the interactions between the incident electron beam and individual atoms in the specimen produce various signals that can be used to determine the elemental composition of the specimen. The irradiated sample atoms emit several characteristic X-ray peaks that can be used to estimate their local concentrations. The deceleration and deflection of the electron beam furthermore produces a continuous X-ray background radiation that can be used to estimate the mass density of the specimen.

It is generally accepted that by ~ 30 h post-invasion the original steep Na^+ and K^+ gradients across the host cell membrane are largely dissipated [34], surrounding the parasite within the host cell with a high-Na, low-K milieu, very similar to that in typical extracellular media. EPXMA has been used to quantify the influence of qinghaosu and chloroquine on the host cell potassium, sodium and phosphorus concentrations [34]. It was observed that these antimalarials reduce parasite phosphorous concentrations, suggesting an arrest of growth. Using EPXMA Rohrbach et al. observed only moderate Ca concentrations in the parasite food vacuole and suggested that it is not a major intracellular Ca^{2+} store [49].

Sample preparation is a very critical step in any EM investigation. Because electron microscopes are operated under high vacuum, water needs to be removed from the specimen. Freezing the cells in liquid propane cooled in liquid nitrogen at specified developmental stages immobilises the elements of interest. The cells are then cryosectioned in the frozen, hydrated state and subsequently freeze-dried to avoid the redistribution of the freely diffusible elements (Na and K) [59]. A thin coating of carbon is applied to improve the stability of the sections during subsequent analysis. In thin sections (100 nm thickness) a lateral spatial resolution of 10–20 nm and a minimum detectable elemental concentration of 1 mmol per kg dry mass can be achieved [18]. The accuracy of this technique depends on several factors, but chiefly on the ability to separate peak from background in the spectrum and the accuracy of the calibration standards used [58]. An accuracy for K of $\pm 1\%$ is possible since this element is plentiful

in the cell and the peaks are well separated. The accuracy for Na is less than this, due to its low concentration and the higher background under this peak, whereas the accuracy for Ca is affected both by its low concentration within the cell and by overlap of its main peak ($\text{Ca}-\text{K}_\alpha$) by a secondary K peak ($\text{K}-\text{K}_\beta$).

Figure 3 shows a sample spectrum of an uninfected and a late stage IRBC, taken in the erythrocyte cytosol (unpublished data from the authors, but see also [34]). The Na peak area is smaller in the uninfected cell spectrum, whereas the K peak is larger, indicating the onset of the

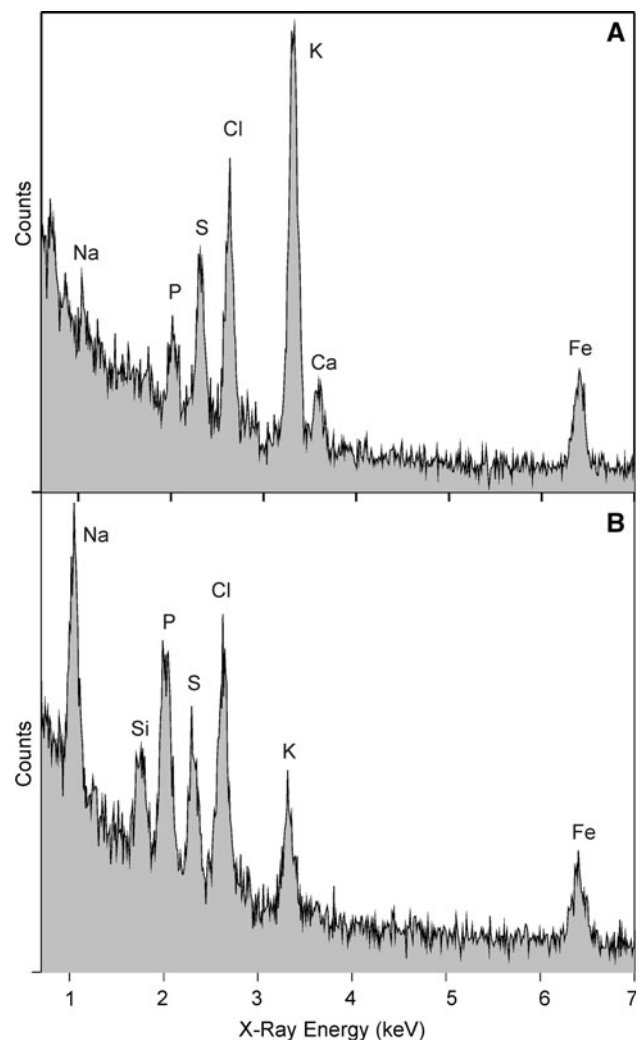


Fig. 3 Change of cytosol composition reported by X-ray microanalysis. (a) Shows a spectrum of an uninfected RBC thin section. The background radiation decays with increasing energies and needs to be subtracted for quantifications. Uninfected RBCs exhibit a large peak area for K and Fe and a much smaller peak area for Na. (b) Shows the host cytosol composition for a trophozoite IRBC. The Na peak area is significantly larger, while K is reduced. The Fe peak area is not very different between uninfected and infected RBC. Other elemental peaks (P, S, Cl, Ca) can be observed, with artifactual Si stemming from the desiccant used during freeze-drying

parasite induced dissipation of the host membrane Na/K gradient.

4 Manipulating IRBCs with light

4.1 Optical tweezers

The elasticity of IRBCs becomes progressively reduced with ongoing parasite maturation and febrile temperatures, with occlusive implications to circulatory rheology. Previous measurements of IRBC elasticity have been done using shear-rheometers [11], micropipette aspiration [45], magnetic twisting cytometry [39], observing membrane fluctuations [46] or using optical tweezers [5]. Optical tweezers have been used to measure the mechanical properties of both healthy and infected cells [54, 55, 60]. It is possible to deform RBCs either by attaching colloidal particles to the membrane, and focusing the laser trap onto the beads, or by directly scanning the laser trap through the cell [7, 26, 52]. In addition to mechanical measurements, optical tweezers can be particularly powerful as a method of micropositioning cells for the investigation of merozoite pre-invasion events [35]. It only takes a few seconds between the instant a merozoite first comes in contact with a red cell targeted for invasion and the instant the merozoite becomes aligned for penetration. During this period, the merozoite-red cell contact triggers dramatic deformations of the cell surface aimed at reorienting the merozoite so that its apical end makes contact with the membrane. This pre-invasion period is one of the least understood stages in malaria invasion. To investigate this period in detail with all the power imaging methodologies can provide it is necessary to configure an experimental system such that the frequency of contacts between recently released merozoites and uninfected red cells is optimized. Merozoite infectivity decreases rapidly with time. Furthermore it would be desirable to have the capability of using fluorescence microscopy imaging at a resolution such that the apical alignment process is resolved at subcellular level. Optical tweezers can be used to achieve this goal by micropositioning a ring of uninfected red cells around a number of IRBCs about to rupture, as illustrated here in Fig. 4 (unpublished data from the authors, but see also [60]).

4.2 Optical stretcher

While micropipette aspiration or optical tweezers both usually require contact with the cells for quantitative single-cell mechanical measurements and are low-throughput, a so called optical stretcher can determine IRBC elasticity in a non-contact mode and with high throughput [24, 40].

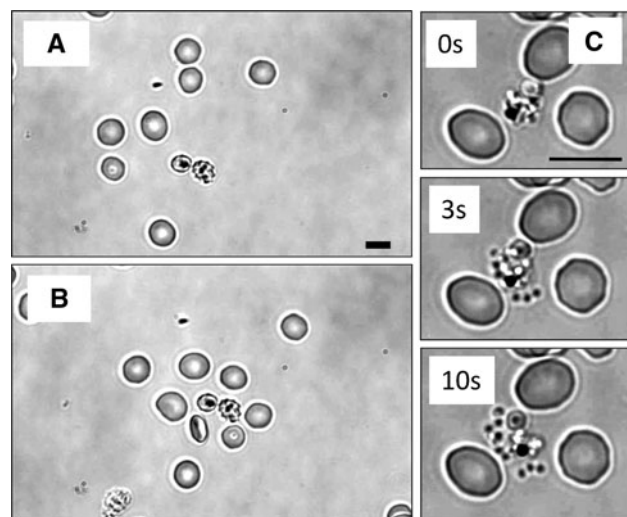


Fig. 4 Use of optical traps for surrounding IRBCs close to rupture with uninjected red cells. (a) Shows the original field configuration with an IRBC in the centre, identified as close to rupture. (b) Shows how an optical trap has been used to corral this IRBC with uninjected RBCs. (c) Shows sequential images from a continuous record of IRBC rupture and merozoite dispersion towards surrounding uninjected red blood cells micropositioned proximally as invasion targets to enable optimal observation of the pre-invasion process

Rather than trapping dielectric particles in the focus of one strongly focused laser beam, as is usually done in optical tweezers, in an optical stretcher objects are trapped between two non-focused counter-propagating laser beams. Figure 5a illustrates the principle setup. It is possible to stretch the trapped cell along the axis of the laser beams simply by modulating the intensity of the light that passes through it and without the need for beads to be attached to the cell surface as handles [25, 33, 48]. The stretching forces are generated by the momentum transfer that occurs at the change in refractive index between the sample cell and the surrounding medium. The refractive index n is directly proportional to the momentum p of light, $p = n \cdot E/c$, where E is the energy of the light and c the speed of light in vacuum. As the light enters or leaves the cell its momentum changes. This results in forces at both surfaces according to Newton's law, which are normal to and directed away from the surface of the cell [23]. These surface forces are pulling the cell apart, much like in a tug-of-war situation, and can be 1–2 orders of magnitude larger than the net trapping forces, which essentially arise from asymmetric distributions of the surface forces [24]. Figure 5b shows an example of optically stretching an uninfected and an infected RBC, plotting the time course of the normalized cell length along the trapping axis.

Optical stretching is a promising novel technique to measure red blood cell membrane mechanical properties. Its main advantage is that it operates entirely in a non-contact manner and can thus render results that are free

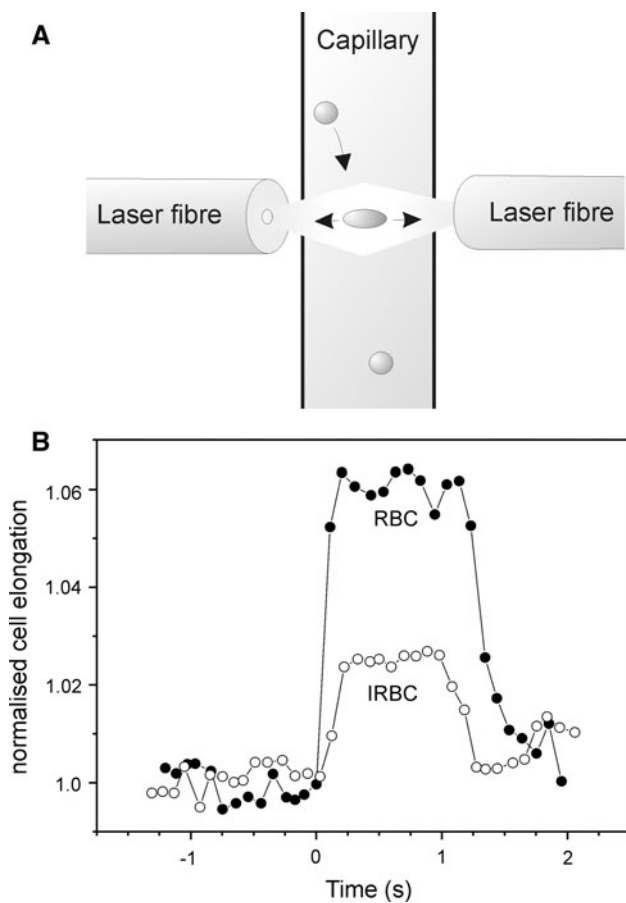


Fig. 5 Optical Stretching of (infected) red blood cells. (a) Sketches the schematics of an optical stretcher setup. A flow capillary passes between two opposing laser fibres. When cells in the capillary are near the trapping region (the geometrical centre of the crossing beams) they are optically lifted into the trap. A step-like modulation of the light intensity elongates the cells. An example cell stretch experiment is depicted in (b). Infected cells are stiffer and thus less deformable in the optical stretcher [40, 54]

from other distortions used in single cell mechanical experiments such as adhering beads at the cell membrane. In addition, by incorporation into a suitable microfluidic environment, throughput rates in excess of 100 cells/h can be achieved, which compares favorably with other single cell mechanical measurement techniques [37, 38].

As an aside, a variant of the optical stretcher is the optical cell rotator, which uses one non-rotationally symmetric laser beam to align red blood cells with respect to their orientation around the optical axis [30]. By slowly rotating this asymmetry, RBCs can be rotated through the focal plane of any microscope (including quantitative phase microscopes, see above) to acquire images from multiple viewing angles. These images can then be used for a tomographic reconstruction, unambiguously decoupling shape changes from changes in refractive index and thus protein concentration.

5 Conclusions

Optical techniques are revolutionizing the way in which biological questions can be addressed directly in the living cell. The use of functional imaging is now widespread in molecular biology but their application in blood disease research is a more recent phenomenon. This article summarizes the development and application of modern microscopic tools that permit detailed investigations of morphological and homeostatic changes occurring in malaria-infected red blood cells. We review the available high-resolution imaging techniques to track and quantify changes in morphology and composition during different stages of the intraerythrocytic cycle of *P. falciparum* and also the optical techniques that inform on the changes in mechanical properties during the infection cycle. Their sensitivity, specificity and non-intrusiveness make optical techniques indispensable to generate high-fidelity data, significantly improving the tools available to future research into blood disease. The combined application of these techniques promises to shed new light on the detailed mechanisms of malaria infection with the hope of finding new diagnostic or therapeutic approaches.

Acknowledgments This study was supported by funds from the EPSRC (EP/E059384), BBSRC (BB/E008542/1) and by a grant from the Isaac Newton Trust to TT. YZ is supported by the Korea Foundation for International Cooperation of Science & Technology (KICOS) through a grant provided by the Korean Ministry of Education Science & Technology (MEST) in 2009 (No. 2009-00591). AE is supported by the Engineering and Physical Sciences Research Council UK (EP/F044011/1).

References

1. Aikawa M (1997) Studies on falciparum malaria with atomic-force and surface-potential microscopes. Ann Trop Med Parasitol 91(7):689–692
2. Aikawa M, Kamanura K, Shiraishi S, Matsumoto Y, Arwati H, Torii M, Ito Y, Takeuchi T, Tandler B (1996) Membrane knobs of unfixed *Plasmodium falciparum* infected erythrocytes: new findings as revealed by atomic force microscopy and surface potential spectroscopy. Exp Parasitol 84(3):339–343
3. Akaki M, Nagayasu E, Nakano Y, Aikawa M (2002) Surface charge of *Plasmodium falciparum* merozoites as revealed by atomic force microscopy with surface potential spectroscopy. Parasitol Res 88(1):16–20
4. Allen RJ, Kirk K (2004) Cell volume control in the Plasmodium-infected erythrocyte. Trends Parasitol 20(1):7–10; discussion 10–1
5. Block SM (1990) Optical tweezers: a new tool for biophysics. In: Grinstein S, Foskett JK (ed) Noninvasive techniques in cell biology. Wiley-Liss, New York, p 375
6. Boutet de Monvel J, Le Calvez S, Ulfendahl M (2001) Image restoration for confocal microscopy: improving the limits of deconvolution, with application to the visualization of the mammalian hearing organ. Biophys J 80(5):2455–2470
7. Bronkhorst PJ, Streekstra GJ, Grimbergen J, Nijhof EJ, Sixma JJ, Brakenhoff GJ (1995) A new method to study shape recovery of

- red blood cells using multiple optical trapping. *Biophys J* 69(5): 1666–1673
8. Choi W, Fang-Yen C, Badizadegan K, Oh S, Lue N, Dasari RR, Feld MS (2007) Tomographic phase microscopy. *Nat Methods* 4(9):717–719
 9. De Cian A, Grellier P, Mouray E, Depoix D, Bertrand H, Monchaud D, Teulade-Fichou MP, Mergny JL, Alberti P (2008) Plasmodium telomeric sequences: structure, stability and quadruplex targeting by small compounds. *ChemBioChem* 9(16): 2730–2739
 10. Degliesposti G, Kasam V, Da Costa A, Kang HK, Kim N, Kim DW, Breton V, Kim D, Rastelli G (2009) Design and discovery of plasmeprin II inhibitors using an automated workflow on large-scale grids. *ChemMedChem* 4(7):1164–1173
 11. Dobbe JG, Hardeman MR, Streekstra GJ, Strackee J, Ince C, Grimbogen CA (2002) Analyzing red blood cell-deformability distributions. *Blood Cells Mol Dis* 28(3):373–384
 12. Elder AD, Domin A, Schierle GSK, Lindon C, Pines J, Esposito A, Kaminski CF (2009) A quantitative protocol for dynamic measurements of protein interactions by Förster resonance energy transfer-sensitized fluorescence emission. *J R Soc Interface* 6: S59–S81
 13. Elder AD, Kaminski CF, Frank JH (2009) phi2FLIM: a technique for alias-free frequency domain fluorescence lifetime imaging. *Optics Express* 17(25):23181–23203
 14. Elliott JL, Saliba KJ, Kirk K (2001) Transport of lactate and pyruvate in the intraerythrocytic malaria parasite, *Plasmodium falciparum*. *Biochem J* 355(Pt 3):733–739
 15. Elliott DA, McIntosh MT, Hosgood HD III, Chen S, Zhang G, Baevoova P, Joiner KA (2008) Four distinct pathways of hemoglobin uptake in the malaria parasite *Plasmodium falciparum*. *Proc Natl Acad Sci USA* 105(7):2463–2468
 16. Esposito A, Chomette J-B, Skepper J, Mauritz JM, Lew VL, Kaminski C, Tiffert T (2010) Quantitative imaging of human red blood cells infected with *Plasmodium falciparum*. *Biophys J* (in press)
 17. Esposito A, Tiffert T, Mauritz JMA, Schlachter S, Bannister LH, Kaminski CF, Lew VL (2008) FRET imaging of hemoglobin concentration in *Plasmodium falciparum*-infected red cells. *PLoS ONE* 3(11):e3780
 18. Fernandez-Segura E, Warley A (2008) Electron probe X-ray microanalysis for the study of cell physiology. *Methods Cell Biol* 88:19–43
 19. Francis LW, Lewis PD, Wright CJ, Conlan RS (2010) Atomic force microscopy comes of age. *Biol Cell* 102(2):133–143
 20. Garcia CR, Takeuchi M, Yoshioka K, Miyamoto H (1997) Imaging *Plasmodium falciparum*-infected ghost and parasite by atomic force microscopy. *J Struct Biol* 119(2):92–98
 21. Glushakova S, Yin D, Li T, Zimmerberg J (2005) Membrane transformation during malaria parasite release from human red blood cells. *Curr Biol* 15(18):1645–1650
 22. Glushakova S, Yin D, Gartner N, Zimmerberg J (2007) Quantification of malaria parasite release from infected erythrocytes: inhibition by protein-free media. *Malar J* 6:61
 23. Guck J, Ananthakrishnan R, Moon TJ, Cunningham CC, Kas J (2000) Optical deformability of soft biological dielectrics. *Phys Rev Lett* 84(23):5451–5454
 24. Guck J, Ananthakrishnan R, Mahmood H, Moon TJ, Cunningham CC, Kas J (2001) The optical stretcher: a novel laser tool to micromanipulate cells. *Biophys J* 81(2):767–784
 25. Guck J, Schinkinger S, Lincoln B, Wottawah F, Ebert S, Romeyke M, Lenz D, Erickson HM, Ananthakrishnan R, Mitchell D, Kas J, Ulwick S, Bilby C (2005) Optical deformability as an inherent cell marker for testing malignant transformation and metastatic competence. *Biophys J* 88(5):3689–3698
 26. Henon S, Lenormand G, Richert A, Gallet F (1999) A new determination of the shear modulus of the human erythrocyte membrane using optical tweezers. *Biophys J* 76(2):1145–1151
 27. Kaminski CF (2005) Fluorescence imaging of reactive processes. *Zeitschrift Fur Physikalische Chemie—Int J Res Phys Chem Chem Phys* 219(6):747–774
 28. Kasas S, Thomson NH, Smith BL, Hansma PK, Miklossy J, Hansma HG (1997) Biological applications of the AFM: from single molecules to organs. *Int J Imaging Syst Technol* 8(2): 151–161
 29. Kirk K (2001) Membrane transport in the malaria-infected erythrocyte. *Physiol Rev* 81(2):495–537
 30. Kreysing MK, Kiessling T, Fritsch A, Dietrich C, Guck JR, Kas JA (2008) The optical cell rotator. *Opt Express* 16(21): 16984–16992
 31. Krugliak M, Zhang J, Ginsburg H (2002) Intraerythrocytic *Plasmodium falciparum* utilizes only a fraction of the amino acids derived from the digestion of host cell cytosol for the biosynthesis of its proteins. *Mol Biochem Parasitol* 119(2):249–256
 32. Kuhn Y, Rohrbach P, Lanzer M (2007) Quantitative pH measurements in *Plasmodium falciparum*-infected erythrocytes using pHluorin. *Cell Microbiol* 9(4):1004–1013
 33. Lautenschlager F, Paschke S, Schinkinger S, Bruel A, Beil M, Guck J (2009) The regulatory role of cell mechanics for migration of differentiating myeloid cells. *Proc Natl Acad Sci USA* 106(37):15696–15701
 34. Lee P, Ye Z, Van Dyke K, Kirk RG (1988) X-ray microanalysis of *Plasmodium falciparum* and infected red blood cells: effects of qinghaosu and chloroquine on potassium, sodium, and phosphorus composition. *Am J Trop Med Hyg* 39(2):157–165
 35. Lew VL, Tiffert T (2007) Is invasion efficiency in malaria controlled by pre-invasion events? *Trends Parasitol* 23(10):481–484
 36. Lew VL, Tiffert T, Ginsburg H (2003) Excess hemoglobin digestion and the osmotic stability of *Plasmodium falciparum*-infected red blood cells. *Blood* 101(10):4189–4194
 37. Lincoln B, Schinkinger S, Travis K, Wottawah F, Ebert S, Sauer F, Guck J (2007) Reconfigurable microfluidic integration of a dual-beam laser trap with biomedical applications. *Biomed Microdevices* 9(5):703–710
 38. Lincoln B, Wottawah F, Schinkinger S, Ebert S, Guck J (2007) High-throughput rheological measurements with an optical stretcher. *Methods Cell Biol* 83:397–423
 39. Marinkovic M, Diez-Silva M, Pantic I, Fredberg JJ, Suresh S, Butler JP (2009) Febrile temperature leads to significant stiffening of *Plasmodium falciparum* parasitized erythrocytes. *Am J Physiol Cell Physiol* 296(1):C59–C64
 40. Mauritz J, Tiffert T, Seear R, Lautenschlager F, Esposito A, Lew V, Guck J, Kaminski CF (2010) Detection of *Plasmodium falciparum*-infected red blood cells by optical stretching. *J Biomed Opt* 15:030517
 41. Mauritz JM, Esposito A, Ginsburg H, Kaminski CF, Tiffert T, Lew VL (2009) The homeostasis of *Plasmodium falciparum*-infected red blood cells. *PLoS Comput Biol* 5(4):e1000339
 42. Mens PF, van Overmeir C, Bonnet M, Dujardin JC, d'Alessandro U (2008) Real-time PCR/MCA assay using fluorescence resonance energy transfer for the genotyping of resistance related DHPS-540 mutations in *Plasmodium falciparum*. *Malar J* 7:48
 43. Nagao E, Kaneko O, Dvorak JA (2000) *Plasmodium falciparum*-infected erythrocytes: qualitative and quantitative analyses of parasite-induced knobs by atomic force microscopy. *J Struct Biol* 130(1):34–44
 44. Nagao E, Nishijima H, Akita S, Nakayama Y, Dvorak JA (2000) The cell biological application of carbon nanotube probes for atomic force microscopy: comparative studies of malaria-infected erythrocytes. *J Electron Microsc* 49(3):453–458

45. Nash GB, O'Brien E, Gordon-Smith EC, Dormandy JA (1989) Abnormalities in the mechanical properties of red blood cells caused by *Plasmodium falciparum*. *Blood* 74(2):855–861
46. Park YK, Diez-Silva M, Popescu G, Lykotrafitis G, Choi WS, Feld MS, Suresh S (2008) Refractive index maps and membrane dynamics of human red blood cells parasitized by *Plasmodium falciparum*. *Proc Natl Acad Sci USA* 105(37):13730–13735
47. Peter M, Ameer-Beg SM (2004) Imaging molecular interactions by multiphoton FLIM. *Biol Cell* 96(3):231–236
48. Remmerbach TW, Wottawah F, Dietrich J, Lincoln B, Wittekind C, Guck J (2009) Oral cancer diagnosis by mechanical phenotyping. *Cancer Res* 69(5):1728–1732
49. Rohrbach P, Friedrich O, Hentschel J, Plattner H, Fink RH, Lanzer M (2005) Quantitative calcium measurements in subcellular compartments of *Plasmodium falciparum*-infected erythrocytes. *J Biol Chem* 280(30):27960–27969
50. Safeukui I, Millet P, Boucher S, Melinard L, Fregeville F, Recveur MC, Pistone T, Fialon P, Vincendeau P, Fleury H, Malvy D (2008) Evaluation of FRET real-time PCR assay for rapid detection and differentiation of Plasmodium species in returning travellers and migrants. *Malar J* 7:70
51. Saliba KJ, Horner HA, Kirk K (1998) Transport and metabolism of the essential vitamin pantothenic acid in human erythrocytes infected with the malaria parasite *Plasmodium falciparum*. *J Biol Chem* 273(17):10190–10195
52. Sleep J, Wilson D, Simmons R, Gratzer W (1999) Elasticity of the red cell membrane and its relation to hemolytic disorders: an optical tweezers study. *Biophys J* 77(6):3085–3095
53. Staines HM, Ellory JC, Kirk K (2001) Perturbation of the pump-leak balance for Na(+) and K(+) in malaria-infected erythrocytes. *Am J Physiol Cell Physiol* 280(6):C1576–C1587
54. Suresh S (2006) Mechanical response of human red blood cells in health and disease: some structure-property-function relationships. *J Mater Res* 21(8):1871–1877
55. Suresh S, Spatz J, Mills JP, Micoulet A, Dao M, Lim CT, Beil M, Seufferlein T (2005) Connections between single-cell biomechanics and human disease states: gastrointestinal cancer and malaria. *Acta Biomater* 1(1):15–30
56. Tokumasu F, Dvorak J (2003) Development and application of quantum dots for immunocytochemistry of human erythrocytes. *J Microsc* 211(Pt 3):256–261
57. Tokumasu F, Fairhurst RM, Osteria GR, Brittain NJ, Hwang J, Wellemes TE, Dvorak JA (2005) Band 3 modifications in *Plasmodium falciparum*-infected AA and CC erythrocytes assayed by autocorrelation analysis using quantum dots. *J Cell Sci* 118(Pt 5): 1091–1098
58. Warley A (1997) X-ray microanalysis for biologists. In: Glauert AM (ed) Practical methods in electron microscopy, vol 16. Portland Press, London and Miami
59. Warley A, Skepper JN (2000) Long freeze-drying times are not necessary during the preparation of thin sections for X-ray microanalysis. *J Microsc* 198(Pt 2):116–123
60. Yoon YZ, Kotar J, Yoon G, Cicuta P (2008) The nonlinear mechanical response of the red blood cell. *Phys Biol* 5(3):36007
61. Zanner MA, Galey WR, Scaletti JV, Brahm J, Vander Jagt DL (1990) Water and urea transport in human erythrocytes infected with the malaria parasite *Plasmodium falciparum*. *Mol Biochem Parasitol* 40(2):269–278